16/06 – 2000

Molecular Modelling of Pd(0) Insertion into Carbon-Halogen Bonds[⋆]

J. M. Jakt

Department of Chemistry, Imperial College of Science, Technology and Medicine, South Kensington, London, SW7 2AY, UK

Abstract:

The oxidative addition of a C-X bond (X = F, Cl, Br, I) to palladium intermediate in the mechanism for the Suzuki synthesis of various biaryl systems has been modelled and investigated computationally using the RHF/3-21G* basis set for *ab initio* calculations in GAMESS (Macintosh version). Mainly variously substituted alkyne halide metal complexes –reactants, transition states, and products– have been used to model much larger (and therefore more time-consuming to calculate) aryl and η^6-tricarbonylchromium(0) aryl complexes. The effects variously of non-substitution, electron-withdrawing groups, and electron-donating groups on the activation energies of the desired products and conformations of the transition states have thus been elucidated.

[⋆] Many thanks due to Dr. Sonsoles Martín-Santamaría, Dr. Henry S. Rzepa and Dr. David A. Widdowson for invaluable help, guidance and advice on the execution of this project.

Introduction:

Biaryl and binaphthyl compounds constitute attractive targets as, amongst others, chiral ligands in asymmetric reactions[1]*, or as biologically active natural products*[2]*. Suzuki couplings which produce such biaryl products currently enjoy considerable attention amongst synthetic chemists*[3]*. The palladium(0) Suzuki cross-coupling reaction is illustrated in* ***Scheme 1***[4]*.*

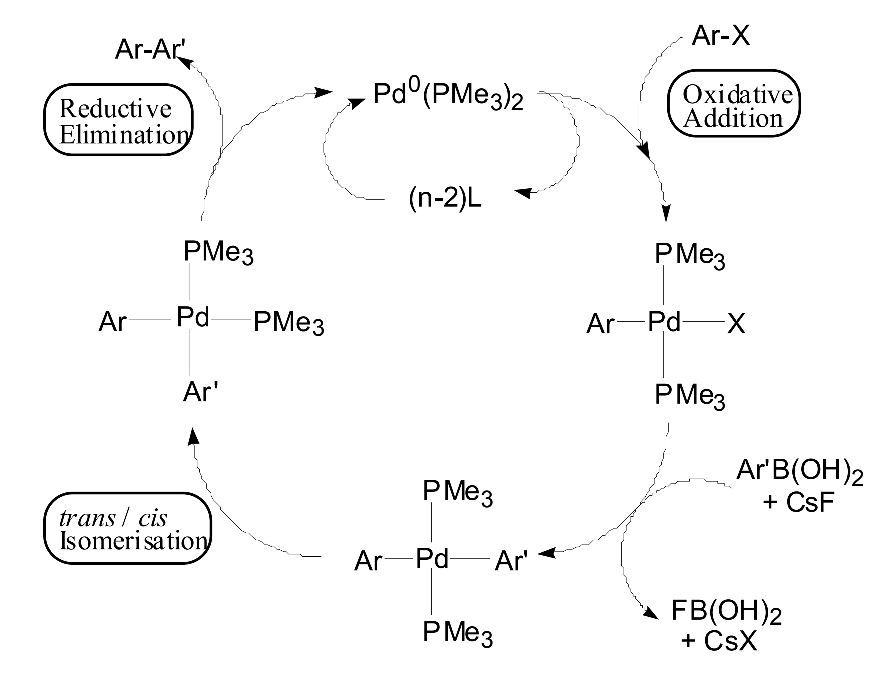

Scheme 1

Some significant developments in recent years in the synthesis of these compounds of note include:

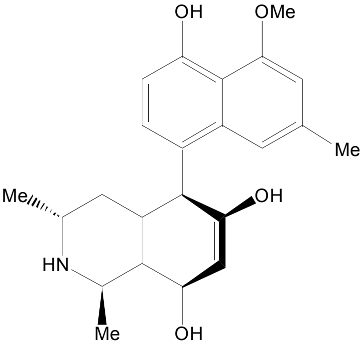

Korupensamine A

Figure 1

Watanabe *et al.*[5] provided an important development to this field in demonstrating diastereoselectivity in the cross-coupling reaction of tricarbonylchromium complexes with binaphthyl compounds related to possible korupensamine anti-malarial candidates derived from the tropical liana *Ancistrocladus korupensis* (**Scheme 2**). A promising strategy to an efficient methodology for the synthesis of enantiomerically pure forms of this series of alkaloids with naphthyl and tetrahydroisoquinoline elements linked by one C-C bond was thus provided. Product **1** was attained in 89% yield without the formation of diastereoisomeric product **2**, and represents a kinetically controlled product with severe steric interaction between the chromium moiety and the *ortho*-substituents next to the central bond of the naphthalene element. It readily isomerises to the thermodynamically more stable axial configuration product **2** in 98% yield upon heating. This diastereoselectivity of reaction can then be usefully employed for the synthesis of more complex aryl coupling products such as those of the korupensamine family (**Figure 1**).

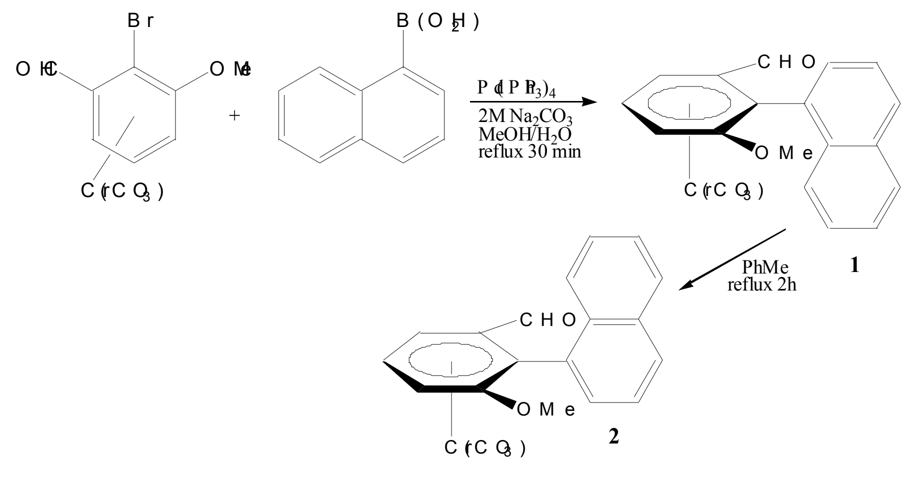

Scheme 2

Kamikawa *et al.*[6] expanded upon this work with a Suzuki-Miyaura palladium cross-coupling of 2,6-disubstituted bromobenzenechromium complexes with various *ortho*-substituted phenylboronic acids and *ortho*-formylphenylboronic acids (**Scheme 3**). The former coupling yielded *syn*-configured products **3** (in 55% to 96% yield) with the *ortho*-alkoxy substituent directed towards the chromium moiety despite severe

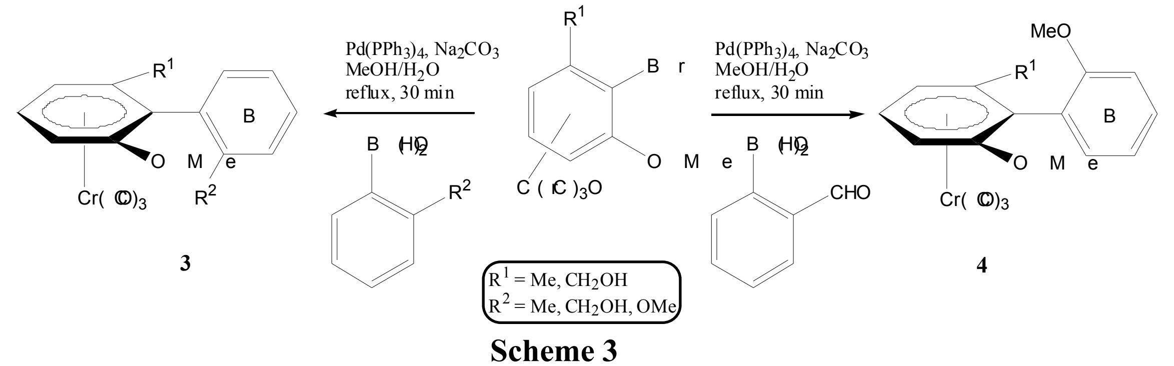

Scheme 3

steric interaction between the two, whilst the latter gave diastereoisomeric *anti*-complexes **4** as the only product under the same conditions (in 43% to 95% yield). As was the case for Watanabe's group, the kinetic *syn*-product (here **3**) was easily isomerised to the more thermodynamically stable *anti*-biphenyl complex (here **4**) by heating under reflux. The rationale for the observed selectivity would appear to involve the formation of highly hindered palladium biaryl transition states where the large palladium substituents will tend to force the steric bulk of the *ortho*-substituents of products **3** away from the palladium, and in the direction of the chromium moiety (**Figure 2**)[7]. The formation of products **4** may then still be favourable due to similar interaction of the formyl group being less unfavourable than that with $Cr(CO)_3$, perhaps due to the generally differing bonding angles of *sp*^{3}-hybridisation over *sp*^{2}-hybridisation.

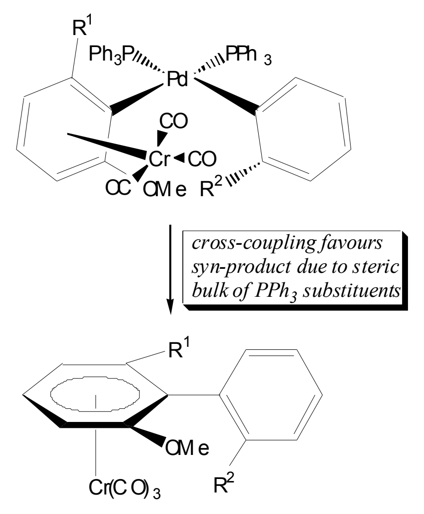

Figure 2

The need for η^6-tricarbonylchromium complexation to aryl halide rings –as described for the reactions above– was triggered by the need to draw electron density out of the aryl ring and thereby weaken the aryl-halide bond[8]. This made cross-coupling more amenable and constituted an especially useful technique for aryl-chlorides as halide partners, which for long were considered inert to this reaction. Indeed, previous to the introduction of this technique the halide reagents for these reactions generally usually only consisted of various aryl iodides and bromides. The technique also benefits from the comparative ease with which the chromium moiety may be de-complexed after cross-coupling. Other means of achieving the same effect included simply adding a conventionally bonded electron-withdrawing group to the ring such as a cyano or trifluoromethyl group[9], or by having a basic phosphine ligand present for palladium[10].

Recently, Widdowson and Wilhelm have expanded upon the use of different aryl halides yet further by the use of aryl fluorides for Suzuki cross-coupling reactions[11].

The group's findings validated an optimal set-up for the palladium catalysed cross-coupling of aryl fluorides as portrayed in **Scheme 4**, effecting yields ranging from 61% to 87% with a variety of arylboronic acids coupled to tricarbonylchromium complexed fluorobenzene rings. Thus substantial evidence suggesting the unprecedented direct participation of fluorobenzene complex in a cross-coupling process via oxidative addition of the C-F bond to the palladium(0) intermediate was attained.

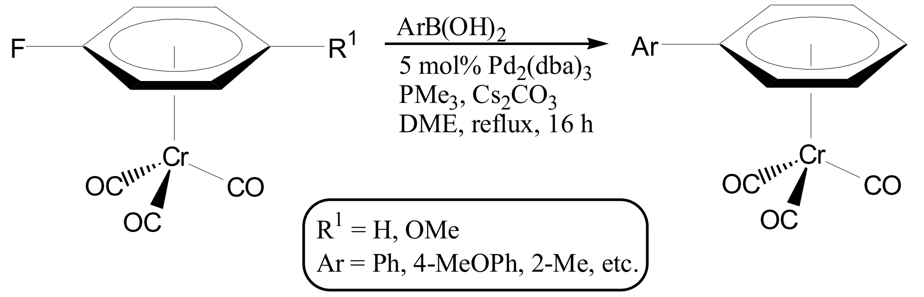

Scheme 4

In the context of this project the point of investigation concerned this latter step of the reaction (**Scheme 5**). It was attempted to gather information regarding the manner and facility of the mechanism and determine whether or not it constitutes a concerted insertion –path (*a*) below–, or an addition-elimination sequence *via* an *exo*-addition of palladium to form **5** followed by the loss of fluoride to yield **6** –path (*b*) below. To this end various alkyne halide pall-adium models –and also ultimately aryl halide palladium models– were used to emulate the more complex Cr $(CO)_3$ aryl system as depict-ed in **Scheme 5**. From a computational point of view this is much more expedient than to attempt the modelling of the fully complexed system

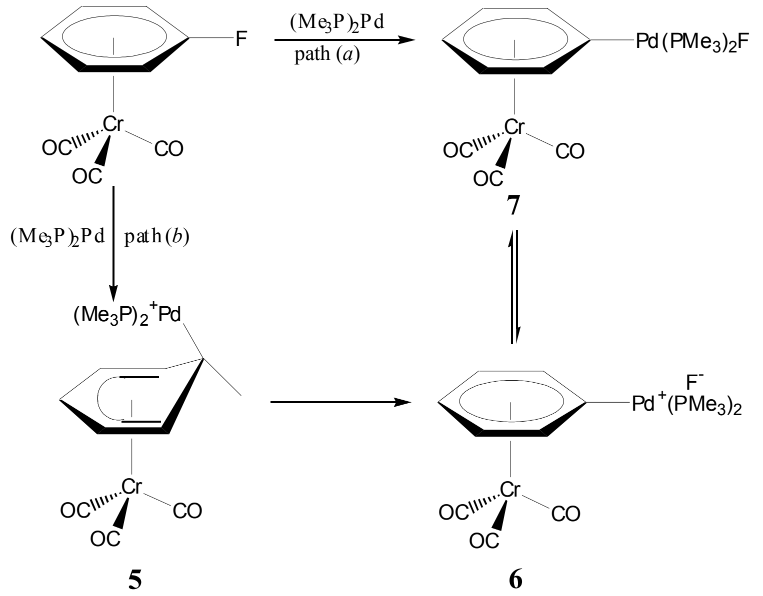

Scheme 5

since the com-putational time and power required would otherwise be debilitating. Since a conventionally bonded electron-withdrawing group is known to have much the same effect as a chromium moiety[8,9], it was judged sufficient to emulate the Cr $(CO)_3$ electron-withdrawing substituents with various electronegative substituents bonded to said alkyne and aryl halides.

Computational Procedure:

The principal tools used were the CAChe (Computer Assisted Chemistry), MacGAMESS and MacMolPlt software (all for Macintosh). CAChe comprises a number of components such as Editor and Visualiser that were used to define initial likely molecular conformations of reactants, transition states and products. These initial species were then transferred to the MacMolPlt programme[12] where they were readied for *ab initio* geometry and energy optimisation calculations in MacGAMESS (The Macintosh implementation of the GAMESS programme[13]) using the 3-21G* basis set[†]. MacMolPlt comprises a graphical interface that can be used to prepare input data for GAMESS, and also to view and examine output data from GAMESS energy and geometry optimisation operations –orbitals, total electron densities and molecular electrostatic potentials can be graphically represented in the programme.

The *ab initio* procedure in GAMESS involves the calculation of orbital wave functions by solving the Schrödinger equation using the Born-Oppenheimer approximation and the Hartree-Fock self-consistent field operator. When running the calculation the starting point is a geometry defined in CAChe and MacMolPlt from which the programme will compute all the integrals guessed from trial coefficients derived from the 3-21G* basis set, and build and diagonalise the determinants and produce a set of orbital energies and first-improved derivatives. This process is then repeated until self-consistency is achieved, in this case defined by the gradient of the first derivatives (GNorm here) converging to 0.0001 Hartrees. This procedure does not take into account correlation energies (electron-electron interactions) or the inherent inaccuracies incurred from deriving electron orbitals from H that result

---

[†] * refers to the inclusion of 1 d heavy atom polarisation function.

especially for other elements such as palladium and the halogens. As a result, the activation barriers calculated for the systems studied in this project are likely to be representative of an upper limit that would probably be brought down if techniques were employed to compensate for these inaccuracies.

The path that the calculations took in determining the heat of formation of the various species could be viewed in MacMolPlt using the associated log files created by MacGAMESS (**Figure 3** ***(d)***). In **Figure 3** the process by which a calculation would

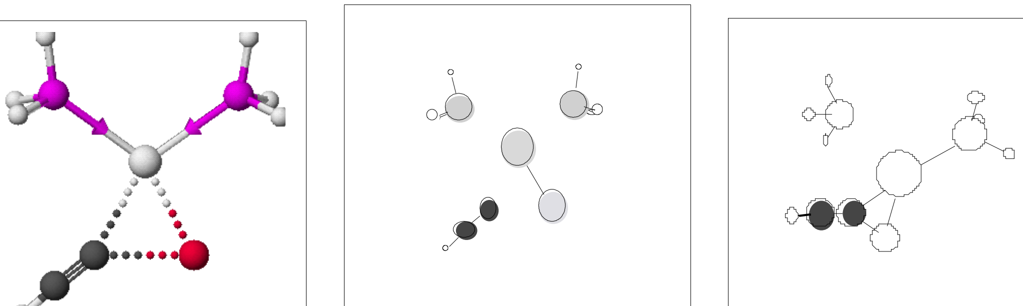

Initial species constructed in Editor.

(a)

Initial species in MacMolPlt, interpreted from CAChe, prior to manipulation in GAMESS.

(b)

Output from GAMESS.

(c)

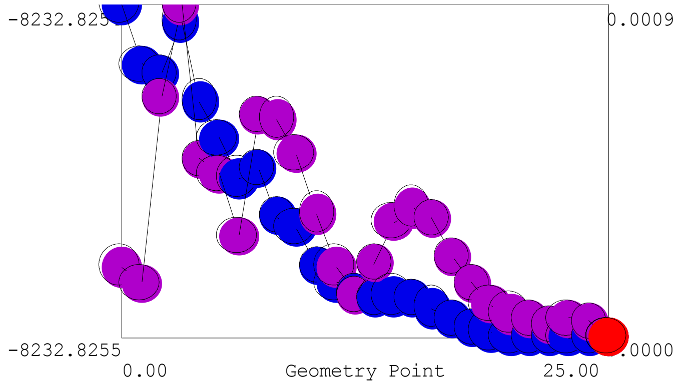

Plot of gradient (GNorm) converging to 0 (purple circles), and Total Energy (blue circle) from MacGAMESS log file

(d)

Figure 3

(a) *represents the initial conformation of the species to be investigated as defined by CAChe (here alkyne bromide complexed to Pd(PH_3)$_2$).* ***(b)*** *represents the same species in MacMolPlt from where a GAMESS input file could be prepared, while* ***(c)*** *and* ***(d)*** *represent GAMESS final output as it appears in MacMolPlt.*

be set up is outlined. First, a configuration thought to be likely for a particular species would be constructed in Editor (**Figure 3*(a)***). This would then be transferred to MacMolPlt (**Figure 3*(b)***) from where it would be processed for optimisation in MacGAMESS, subsequent to which the energy of formation of a particular species could be established. As can be seen from **Figure 3 *(c)***, the initial species constructed in Editor need not necessarily correspond very precisely with the optimised output derived from MacGAMESS.

The input files for the calculation of heats of formation of transition states differed in their preparation to what was the case for the calculations involving ground states of the reactants and products. In **Figure 4** a facsimile of an input file for a transition state is illustrated as it would appear in a simple editing programme such as BBEdit Lite. The points where such a file would differ from that of an input file for ground states are indicated.

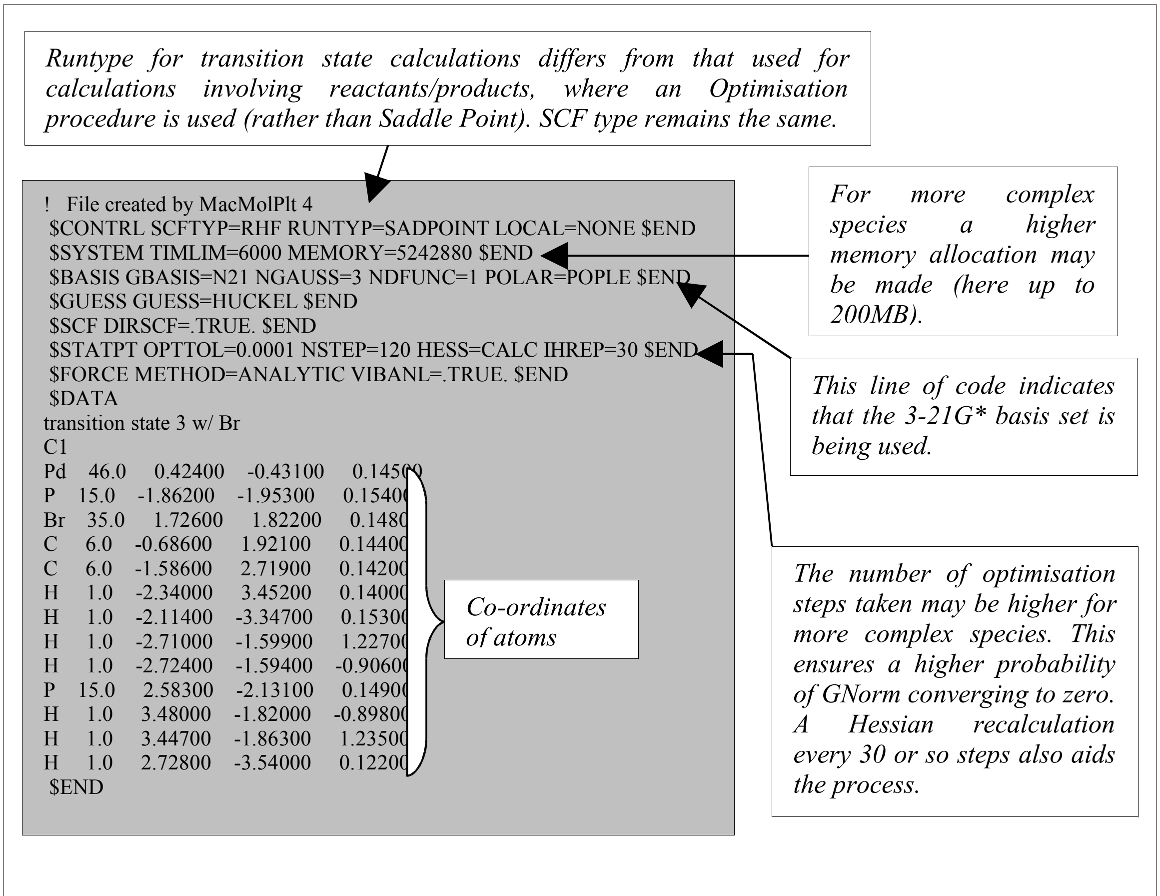

Runtype for transition state calculations differs from that used for calculations involving reactants/products, where an Optimisation procedure is used (rather than Saddle Point). SCF type remains the same.

```
!   File created by MacMolPlt 4
 $CONTRL SCFTYP=RHF RUNTYP=SADPOINT LOCAL=NONE $END
 $SYSTEM TIMLIM=6000 MEMORY=5242880 $END
 $BASIS GBASIS=N21 NGAUSS=3 NDFUNC=1 POLAR=POPLE $END
 $GUESS GUESS=HUCKEL $END
 $SCF DIRSCF=.TRUE. $END
 $STATPT OPTTOL=0.0001 NSTEP=120 HESS=CALC IHREP=30 $END
 $FORCE METHOD=ANALYTIC VIBANL=.TRUE. $END
 $DATA
transition state 3 w/ Br
C1
Pd   46.0    0.42400   -0.43100    0.14500
P    15.0   -1.86200   -1.95300    0.1540
Br   35.0    1.72600    1.82200    0.148
C     6.0   -0.68600    1.92100    0.1440
C     6.0   -1.58600    2.71900    0.1420
H     1.0   -2.34000    3.45200    0.1400
H     1.0   -2.11400   -3.34700    0.1530
H     1.0   -2.71000   -1.59900    1.2270
H     1.0   -2.72400   -1.59400   -0.9060
P    15.0    2.58300   -2.13100    0.1490
H     1.0    3.48000   -1.82000   -0.8980
H     1.0    3.44700   -1.86300    1.2350
H     1.0    2.72800   -3.54000    0.1220
 $END
```

Co-ordinates of atoms

For more complex species a higher memory allocation may be made (here up to 200MB).

This line of code indicates that the 3-21G basis set is being used.*

The number of optimisation steps taken may be higher for more complex species. This ensures a higher probability of GNorm converging to zero. A Hessian recalculation every 30 or so steps also aids the process.

Figure 4

Once found, MacGAMESS can also be used to characterise transition states by calculating the vibrational frequencies of a relevant species using a Hessian calculation. Since there should only be one frequency that corresponds to a negative force constant this can also therefore be used to verify that the programme has found a species that actually is a transition state. This vibrational frequency is shown for a nitro-substituted alkyne fluoride palladium phosphine transition state complex in **Figure 5**. An input file for a Hessian calculation differs in the run type chosen – Hessian– and has no optimisation steps (see **Figure 4**) since the form of the transition state has already been established.

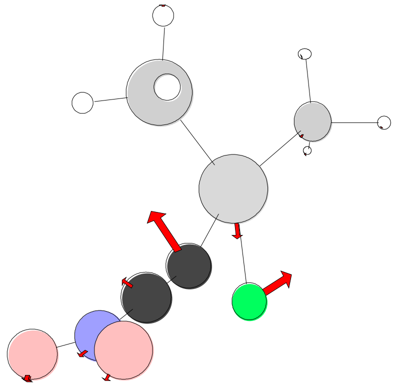

Figure 5

Diagram depicting the vibrational frequency corresponding to the negative force constant of the transition state. The arrows represent movement vectors in the transition state mode.

The strategy for the investigation of the oxidative addition of the C-F bond to the palladium(0) intermediate was initially to emulate an aryl halide with a significantly smaller alkyne halide (**Figure 6**, where R = H). This was then coupled with a putative $Pd(PH_3)_2$ reactant intended to mimic the behaviour of $Pd(PMe_3)_2$ as used experimentally[11] (**Figure 6*(b)***). This initial set-up was felt to give a good approximation to the make-up of electron density and molecular conformation present in the full aryl halide palladium phosphine system. As yet, these experiments did not really attempt to model the electron-withdrawing effects of tricarbonyl chromium complexation, but were instead intended to give an overview as to the extent and range of activation barriers present for the various model systems.

These unsubstituted alkyne models served as a useful control to variously substituted alkyne models, such as that activation barriers could usefully be compared. Substitution was introduced simply by introducing various functional groups in the R-position in **Figure 6**.

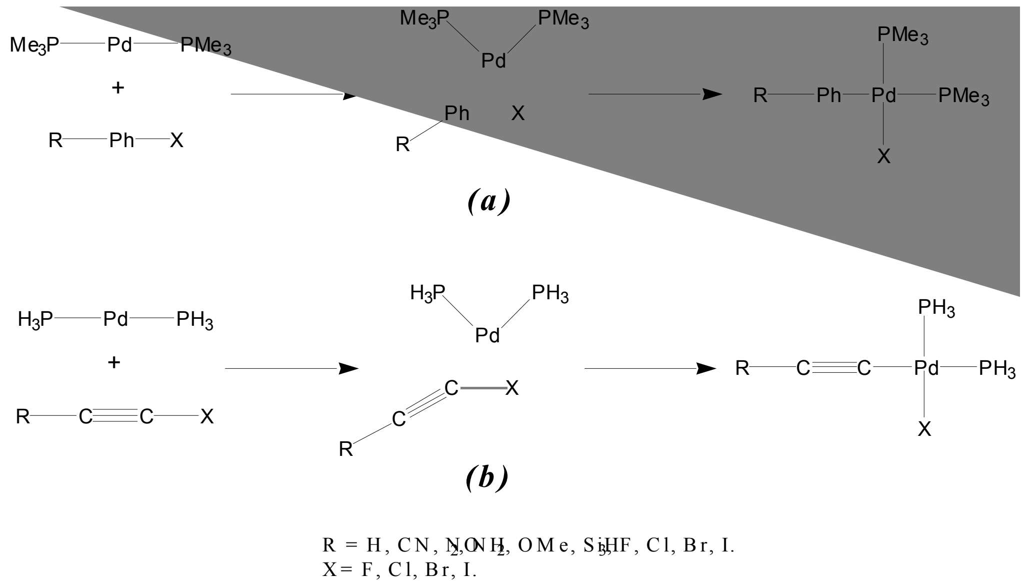

Figure 6

(a) *represents the experimentally correct form of reaction system that was emulated by the system represented in* ***(b)****. Thus PH_3 groups replaced experimentally correct PMe_3 groups on the palladium, and substituted and unsubstituted alkyne halides replaced similarly configured aryl halides. The R groups were used to introduce electron-withdrawing or electron-donating properties to the system.*

The soundness of the alkyne halide palladium phosphine model was ultimately validated by running *ab initio* calculations for unsubstituted alkyne fluoride coupled to experimentally more correct $Pd(PMe_3)_2$, for unsubstituted and cyano-substituted phenyl fluorides coupled to $Pd(PH_3)_2$, and finally for an unsubstituted phenyl fluoride coupled to $Pd(PMe_3)_2$. It was thus endeavoured to test the suitability and accuracy of emulating aryl rings with alkynes and $Pd(PMe_3)_2$ groups with $Pd(PH_3)_2$ groups.

Results and Discussion:

The tables below show the results obtained from the *ab initio* methods for finding the heats of formation of reactants, transition states, and products for the alkyne halide complexes, as well as results from models constructed with aryl halides. Finally, experimental results for an unsubstituted aryl fluoride coupled to $Pd(PMe_3)_2$ are presented.

Palladium reactants:

Palladium reactant:	Heat of formation (hartrees)
$Pd(PH_3)_2$	–5596.7587
$Pd(PMe_3)_2$	–5829.7500

Alkyne Halides of general form:

$R-C\equiv C-X$

R	X	Halide reactant (hartrees)	Transition state (hartrees)	Product (hartrees)	Activation energy[Ψ] (kcal/mol)
H	F	–174.6929	–5771.3991	–5771.4790	32.9
	Cl	–533.2077	–6129.9337	–6130.0123	20.5
	Br	–2636.0775	–8232.8255	–8232.8923	6.7
	I	–6963.7206	–12560.4770[*]	–12560.5280	1.4
CN	F	–265.9106	–5862.6374	–5862.7091	20.0
	Cl	–624.4246	–6221.1646[*]	–6221.2375	11.7
	Br	–2727.2958	–8324.0499[*]	–8324.1174	2.9
	I	–7054.9390	–12651.6886[*]	–12651.7539	5.7
NO_2	F	–376.9494	–5973.6910	–5973.7552	10.7
NH_2	F	–229.4155	–5826.1241	–5826.2030	31.4
OMe	F	–287.9291	–5884.6365	–5884.7228	32.2
SiH_3	F	–463.3576	–6060.0704	–6060.1433	28.8
F	F	–272.9786	–5869.6934[*]	–5869.7776	27.5
Cl	F	–631.5015	–6228.2129	–6228.2948	29.7
Br	F	–2734.3722	–8331.0843	–8331.1646	29.2
I	F	–7062.0171	–12658.7297	–12658.8073	28.9

[Ψ] For calculation of E_A: {[energy, transition state] – [energy, (sum of ground state reactants)] × 627.5}

[*] These values were found to constitute invalid transition states after Hessian analysis. However, the anomalous negative force constants that many of these species are subject to are for the most part of fairly low intensity. Values quoted are from best attempted transition state optimisation procedures.

Alkyne fluoride with $Pd(PMe_3)_2$ coupling partner:

Reaction is: 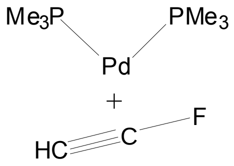	**Reactant (hartrees)**	**Transition state (hartrees)**	**Product (hartrees)**	**Activation energy (kcal/mol)**
	–174.6929	–6004.3991	–6004.4818	27.5

Aryl fluorides with $Pd(PH_3)_2$ coupling partner

Reaction is: 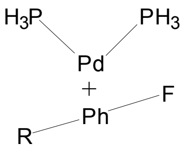	**R**	**Reactant (hartrees)**	**Transition state (hartrees)**	**Product (hartrees)**	**Activation energy (kcal/mol)**
	H	–327.7439	–5924.4321	–5924.4821	44.2
	Para-CN	–418.9609	–6015.6575	–6015.7035	39.0
	Ortho-CN	–418.9602	–6015.6621	–6015.7104	35.6

Aryl fluoride with $Pd(PMe_3)_2$ coupling partner

Reaction is: 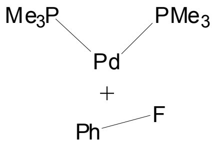	**Reactant (hartrees)**	**Transition state (hartrees)**	**Product (hartrees)**	**Activation energy (kcal/mol)**
	–327.7439	–6157.4322625	–6157.4961	38.7

The reactions generally proceeded via transition states that could be verified from Hessian calculations wherein if only one vibrational frequency of a negative value was found, then the transition state geometry arrived at by MacGAMESS was considered legitimate. For the models where the halogen involved was fluoride all the transition states were of a similar geometry irrespective of substitution to the alkyne (**Figure 7**

(a), where the alkyne fluoride is subject to SiH_3-substitution). Generally one phosphine group adjacent to the fluoride has a bond length to the palladium some 0.3-0.4Å longer than the phosphine group furthest away from the fluoride, which is attributable to electronic repulsion by the palladium-fluoride bond. As regards the fluoride products, similar traits were observed though to a much lesser extent, and the extension of the palladium-phosphine bond *cis* to the fluoride varies from non-existent to at most 0.1Å (**Figure 7*(b)***). Other than this slight variation the products tended to exhibit a symmetrical arrangement of substituents around the palladium such as to minimise steric effects resulting from the bulk of the phosphine ligands and the alkyne system. Similar behaviour was observed in products of alkyne halides constructed with the bigger halogens, and indeed in the larger species constructed with aryl fluorides and/or $Pd(PMe_3)_2$ substituents where the difference in bond length was at most 0.2Å.

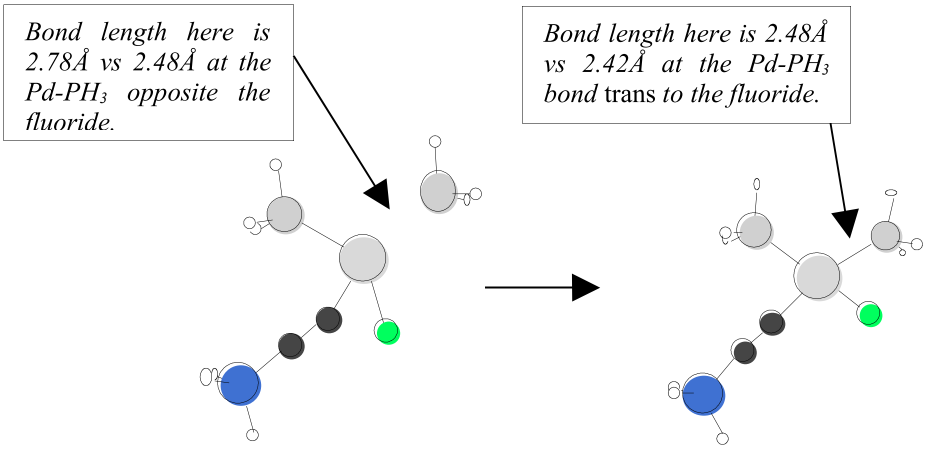

Bond length here is 2.78Å vs 2.48Å at the Pd-PH_3 opposite the fluoride.

Bond length here is 2.48Å vs 2.42Å at the Pd-PH_3 bond trans *to the fluoride.*

(a) ***(b)***

Figure 7

(a) *here represents the transition state for SiH_3-substituted alkyne fluoride coupled with $Pd(PH_3)_2$.*
(b) *represents the ground state product of this process.*

As was to be expected, the effect of changing the halogen component in the alkyne halide from a fluorine to a higher halogen such as chlorine or bromine has the effect of lowering the activation energy for the coupling reaction. This is likely so due to the less electronegative substituent halogen forming a weaker bond to palladium that is more susceptible to nucleophilic substitution by the metal. However, the geometries for the transition states arrived at for the alkyne chloride and alkyne bromide transition states differed markedly from that of the alkyne fluoride (**Figure 8** ***(a)*** and ***(b)*** respectively).

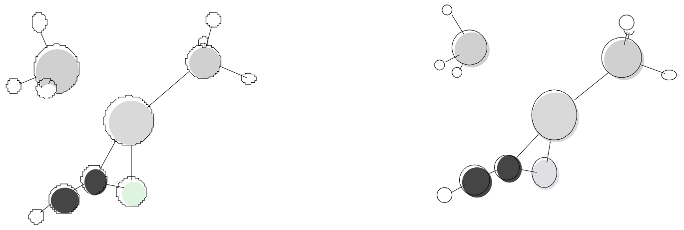

(a) *Alkyne chloride Pd(PH$_3$)$_2$ transition state* ***(b)*** *Alkyne bromide Pd(PH$_3$)$_2$ transition state*

Figure 8

As a higher halogen is added to the model it becomes more twisted and the phosphine group *opposite* the halide now begins to dissociate from the overall structure, ending up outside of the plane of the other substituents, and pointing in towards the electron density of the alkyne. This differs markedly from the behaviour of the alkyne fluoride species where the substituents all stay in the same plane, and may be indicative of some π-bonding interaction on the part of the phosphine with the alkyne body. Interestingly the trend observed for the alkyne fluoride phosphine-palladium bond lengths is also thus reversed. This can in part be explained by the decreased electronic repulsive effects experienced by the phosphines vis-à-vis a 'softer' and less electronegative halide-metal bond.

A transition state was not successfully found for the alkyne iodide, and the structure for which a heat of formation is quoted in the results tables above probably bears only a vague resemblance to a valid transition state. The Hessian calculations for the species did not result in a negative force constant and so the structure is probably not worth modifying any further for the purposes of extrapolating a sound transition state. It may be that the activation energy barrier is simply too low for a transition state to be defined, and, together with the geometries that MacGAMESS tended to favour for the alkyne iodide species, this would then point towards the reaction proceeding *via* an addition-elimination sequence (**Scheme 5**). **Figure 9** illustrates the iodide species as MacGAMESS optimised it and the iodine is here clearly bonded to the alkyne rather than the palladium as would be expected in this case. Further investigation continues into this matter.

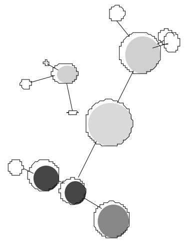

Figure 9

The substitution of an electron-withdrawing group to the modelled alkyne system was intended to give a good approximation of the effect a tricarbonyl chromium moiety would have on an aryl ring. As was anticipated this resulted in a species with a lower activation energy barrier than the unsubstituted system, which is probably due to a withdrawal of electron density from the alkyne system weakening the halide bond in the same way that introducing a higher halogen to the system was observed to do previously. The most notable effect to this end was achieved by introducing NO_2 as a substituent on the alkyne system.

The CN-ligand was used to compare a substituted alkyne system with the full range of halogens as had been done for the unsubstituted system. The transition states were again rather difficult to define for the higher halogens, and in fact only the fluoride was found exactly, since for the chloride and bromide a number of anomalous negative force constants of low intensity were found, as was the case somewhat more significantly for the iodide. Thus the optimised chloride and bromide species are judged to be fairly close to the structure of the actual transition states, while that of iodide is less reliable.

Again a downwards trend is observable in the activation energies as the halogens become bigger, although the trend is seemingly broken for the iodide as the barrier apparently here goes up relative to the bromide. Whether this is due to the inaccuracy of the transition state calculation or whether this is again indicative of there not existing a transition state for the iodide –as may be the case for the unsubstituted alkyne– is open to conjecture. The barrier can not of course go much below

2.9kcal/mol (the value for the cyano-substituted alkyne bromide $Pd(PH_3)_2$ complex), and since the calculations have been carried out with out taking into account correlation energies, the actual values may in fact be *below* these. The geometries of these transition states differ substantially from those for the unsubstituted complexes, being much less twisted and more in the same plane (**Figure 10**).

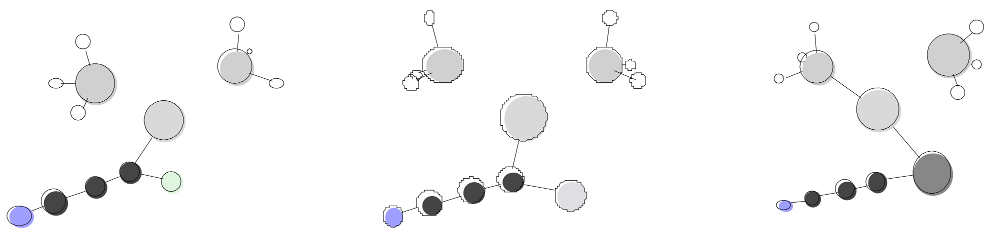

***(a)** CN-Cl-Pd(PH_3)$_2$ trans. state* ***(b)** CN-Br-Pd(PH_3)$_2$ trans. state* ***(c)** CN-I-Pd(PH_3)$_2$ trans. state*

Figure10

Electron-donating groups seemed to have little effect of any significance on activation energy barriers, which is contrary to what might be expected from providing more electron density to the halide bond. This can tentatively be ascribed to the effect differing substituent groups will have on molecular orbitals. Whereas an electron-withdrawing group will tend to interact with the carbon-halogen bond and lower the LUMO of the system, thereby stabilising it, an electron-donating group will here still be too low down energetically to make any difference to the LUMO of the system, and so little interaction with respect to reaction dynamics occurs.

The applicability of the alkyne halide model to emulating aryl halides experimentally was ultimately tested in a final series of long and computationally intensive calculations. First the unsubstituted alkyne fluoride was discarded in favour of an aryl fluoride and this then coupled to $Pd(PH_3)_2$ in order to investigate what difference to the activation barrier this would entail. This was then repeated with *para*- and *ortho*-cyano substituted aryl fluorides coupled to the palladium reagent. The somewhat higher barriers calculated for these aryl complexes as compared with the corresponding alkyne models was thought to be due to the more extensive electron density of the phenyl ring effecting a stronger bond to fluorine. The *ortho*-cyano substituted complex produced the lowest activation barrier result, as would be predicted from a configuration where the electron-withdrawing group is placed closest to the halide bond.

Replacing the PH_3 groups on the palladium reactant with PMe_3 groups had the effect of reducing the barrier height, although not as much as the presence of an aryl reactant had in increasing it. Nevertheless, the validity of using variously substituted alkyne halides to emulate aryl halides did seem to be justified by these results taken in conjunction. For instance, the unsubstituted alkyne fluoride complexed with $Pd(PH_3)_2$ has a calculated activation barrier of 33kcal/mol, which compares with an activation barrier of 44.2kcal/mol for the phenyl fluoride complexed to $Pd(PH_3)_2$. If one takes into account that in reality the coupling would occur with $Pd(PMe_3)_2$, then that suggests that this should be corrected downwards approximately 5kcal/mol. The results for the alkyne model then becomes quite acceptable.

The final calculation for a fully $Pd(PMe_3)_2$ complexed aryl fluoride yielded an activation energy result of 38.7kcal/mol, which compares rather favourably with the value yielded from the much simpler model.

The aryl fluoride $Pd(PMe_3)_2$ transition state (**Figure 11**) and to a lesser extent also the product complex displayed some rather interesting conformational features with regard to its phosphine substituents. It appears that the PMe_3 group adjacent to the fluoride, while possessing a Pd-PMe_3 bond approximately 0.5Å longer than the PMe_3 group opposite the fluoride, at the same time experiences some kind of attractive force vis-à-vis the methyl groups on the phosphorous atom. The same effect can be seen in the product output (**Figure 12**). In addition, on the transition state the methyl groups seem located on the phosphorous atom almost in a sawhorse configuration rather than the expected tetrahedral arrangement. Going back to the transition state, and being able to view the molecule in a 'space-filling' mode in Chem3D (Macintosh variant) with the Van-der-

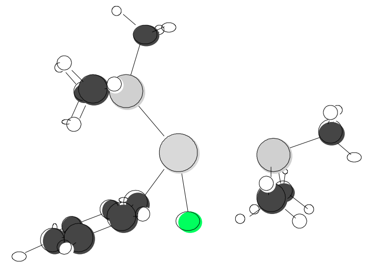

Figure 11

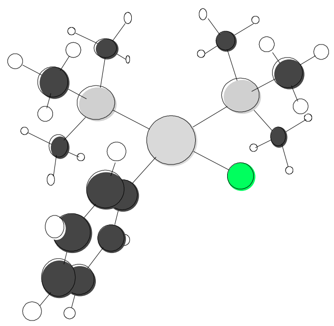

Figure 12

Waalds radii fully filled out (**Figure 13**), there appears to be an optimal space for the fluoride nestled between the adjacent PMe_3 group and the aryl group. The substituents do not seem to be repelling each other here and the PMe_3 substituent appears instead to interact with the fluoride, perhaps with electron density being donated to the fluoride bond from the methyl groups on the phosphorous. This conformation could have profound diastereoselective effects on the cross-coupling reaction overall if a tricarbonyl chromium entity were to be complexed to it. Such an element would be complexed from the same face as the fluoride (the PMe_3 group opposite the fluoride would deter it from complexation from that side), and any cross-coupling substituent would have to approach from the opposite side due to the considerable steric hindrance it would otherwise encounter. It does not seem likely either that the space in which the fluorine atom resides could easily hold any bigger halogen such as Cl or Br.

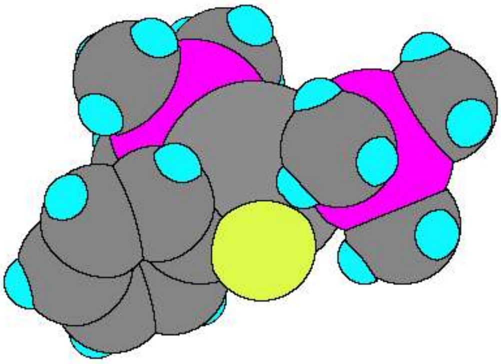

Colour scheme:
green/yellow = F
light blue = H
pink = P
grey = C and Pd

Figure 13

Conclusion:

In having shown that the alkyne halide model coupled with a simplified palladium phosphine can adequately model the much more complex aryl halide system coupled with an experimentally correct palladium phosphine, it has been possible to model the effect of a number of functional groups on the oxidative addition of the carbon-halide bond to a palladium intermediate within the context of the Suzuki cross-coupling reaction. As predicted, the presence of an electron-withdrawing group was shown to dramatically reduce activation energies such as that previously untenable reactions might become experimentally possible to execute in practice. As such, the experiments have validated the significance of including the presence of electron-withdrawing groups such as $Cr(CO)_3$ for cross-coupling reactions, since this aids a weaker carbon-halogen bond. It should also be noted that the absence of correlation energy theory in these calculations mean that more refined calculations should enable somewhat lower activation energies to be calculated.

The experiments have unearthed a number of unexpected features from the coupling reaction especially with higher halides in where the seeming absence of transition states (or rather difficulty in attaining them) indicate that the oxidative addition of the carbon-halide bond may differ in mechanism between lower halides (i.e. F, Cl) to that of higher halides (i.e. Br, I) (see **Scheme 5**). Evidence pointing towards a concerted addition mechanism for aryl/alkyne fluorides (path ***(a)*** in **Scheme 5**) include the unchanging nature of the activation barriers for the reaction with alkyne fluorides substituted with electron-donating groups (such as SiH_3, OMe or NH_2). If the mechanism were an addition-elimination sequence such as outlined in **Scheme 5**, path ***(b)***, then one would expect a more profound effect on the activation barrier in line with the ionic nature of the mechanism wherein an electron-donating group would hinder the reaction.

Evidence pointing towards the addition-elimination sequence of reaction derives from the unexpected geometries and very low activation barriers of the alkyne bromides and iodides in reaction. Here, there are indications that there is a π-complex formation between the alkyne/aryl substituent and the metal prior to product formation, which indicates the validity of the addition-elimination sequence.

References:

1.) *e.g.*: (*a*) A. C. Spivey, T. Fekner, S. E. Spey and H. Adams, 1999, **64**, 9430; (*b*) T. Hayashi, *J. Organomet. Chem.*, 1999, **576**, 195; (*c*) K. Nozaki, N. Sakai, T. Nanno, T. Higashijima, S. Mano, T. Horiuchi, and H. Takaya, *Journal of the American Chemical Society*, 1997, **119**, 4413.

2.) *e.g.*: (*a*) K. Kamikawa, T. Watanabe, A. Daimon and M. Uemura, *Tetrahedron*, 2000, **56**, 2325; (*b*) K. C. Nicolaou, H. Li, C. N. C. Boddy, J. M. Ramanjulu, T. Yue, S. Natarajan, X. Chu, S. Bräse and F. Rübsam, *Chem. -Eur. J.*, 1999, **5**, 2584; (*c*) D. E. Zembower and H. P. Zhang, *J. Org. Chem.*, 1998, **63**, 9300.

3.) *e.g.*: S. P. Stanforth, *Tetrahedron*, 1998, **54**, 263.

4.) I. K. Sebhat, *Ph.D. thesis*, Imperial College, London, 1996.

5.) T. Watanabe, K. Kamikawa and M. Uemura, *Tetrahedron Lett.*, 1995, **36**, 6695.

6.) K. Kamikawa, T. Watanabe, A. Daimon and M. Uemura, *Tetrahedron*, 1999, **56**, 2325.

7.) I. K. Sebhat, *Ph.D. thesis*, Imperial College, London, 1996.

8.) W. J. Scott, *J. Chem. Soc., Chem. Commun.*, 1987, 1755.

9.) K.-i. Gouda, E. Hagiwara, Y. Hatanaka and T. Hiyama, *J. Org. Chem.*, 1996, **61**, 7232.

10.) A. F. Littke and G. C. Fu, *Angew. Chem. Int. Ed.*, 1998, **37**, 3387.

11.) D. A. Widdowson and R. Wilhelm, *Chem. Commun.*, 1999, 2211.

12.) B. M. Bode and M. S. Gordon, *J. Mol. Graphics Mod.*, 1998, 133.

13.) M. W. Schmidt, K. K. Baldridge, J. A. Boatz, S. T. Elbert, M. S. Gordon, J. H. Jensen, S. Koseki, N. Matsunaga, K. A. Nguyen, S. Su, T. L. Windus, M. Dupuis and J. A. Montgomery, *J. Comput. Chem.*, 1993, **14**, 1347.